Biol Cybern (2007) 96:147–163
DOI 10.1007/s00422-006-0109-1

ORIGINAL PAPER

Biological Cybernetics

Kinematic invariants during cyclical arm movements

Natalia Dounskaia

Received: 8 April 2004 / Accepted: 6 September 2006 / Published online: 10 October 2006

Abstract It has been observed that the motion of the arm end-point (the hand, fingertip or the tip of a pen) is characterized by a number of regularities (kinematic invariants). Trajectory is usually straight, and the velocity profile has a bell shape during point-to-point movements. During drawing movements, a two-thirds power law predicts the dependence of the end-point velocity on the trajectory curvature. Although various principles of movement organization have been discussed as possible origins of these kinematic invariants, the nature of these movement trajectory characteristics remains an open question. A kinematic model of cyclical arm movements derived in the present study analytically demonstrates that all three kinematic invariants can be predicted from a two-joint approximation of the kinematic structure of the arm and from sinusoidal joint motions. With this approach, explicit expressions for two kinematic invariants, the two-thirds power law during drawing movements and the velocity profile during point-to-point movements are obtained as functions of arm segment lengths and joint motion parameters. Additionally, less recognized kinematic invariants are also derived from the model. The obtained analytical expressions are further validated with experimental data. The high accuracy of the predictions confirms practical utility of the model, showing that the model is relevant to human performance over a wide range of movements. The results create a basis for the consolidation of various existing interpretations of kinematic invariants. In particular, optimal control is discussed as a plausible source of invariant characteristics of joint motions and movement trajectories.

Keywords Arm movement · Kinematics · Power law · Velocity profile · Trajectory · Curvature

N. Dounskaia (✉)
Movement Control and Biomechanics Lab,
Department of Kinesiology, Arizona State University,
P.O. Box 870404, Tempe, AZ 85287-0404, USA
e-mail: natalia.dounskaia@asu.edu

1 Introduction

During arm movements, the trajectory of the end-point (the hand or the tip of the index finger or a pen) is characterized by a number of consistent kinematic characteristics observed during various direction, amplitude, speed, and load conditions. For instance, end-point trajectory is usually close to a straight line, whereas the velocity profile has a bell shape during point-to-point movements (Georgopoulos et al. 1981; Morasso 1981; Nelson 1983; Soechting and Lacquaniti 1981). Further, there is a relationship between end-point velocity and trajectory curvature when subjects draw elliptical shapes (Lacquaniti et al. 1983; Viviani and Terzuolo 1982). This relationship was described as a two-thirds power law in terms of angular velocity and as a one-third power law in terms of tangential velocity

$$V = \frac{K}{C^{1/3}}. \quad (1)$$

Here V is tangential velocity of the end-point and C is trajectory curvature. The coefficient K, which is often referred to as a *gain factor*, is nearly constant. To avoid confusion, the term "power law" will be used in reference to relationship (1). Although the power law has also been considered in a more general form (Viviani and Flash 1995); here, considerations will be limited to

the commonly used form (1). The straight trajectory, the bell-shaped velocity profile, and the power law will be further referred to as kinematic invariants (KIs).

Although the KIs are consistent characteristics of end-point motion, they are not absolute, as illustrated by the multiple examples demonstrating their violations. For instance, the gain factor K varies during handwriting and drawing movements across movement segments, depending on the size and eccentricity of the elliptical shapes drawn (Lacquaniti et al. 1983; Sternad and Schaal 1999; Viviani and Cenzato 1985; Viviani and Terzuolo 1982). While studying drawing movements in children between 5 and 12 years of age, Viviani and Schneider (1991) found age-dependent differences in K. During point-to-point movements in the sagittal plane, Atkeson and Hollerbach (1985) observed straighter movements in the horizontal (anterioposterior) direction than in the vertical (longitudinal) direction. In addition to movement direction, increases in movement amplitude were also shown to cause deviations from a straight trajectory (Haggard and Richardson 1996; Pollick and Ishimura 1996).

Reasons underlying the KIs and their violations have been the focus of extensive research. In some studies, the KIs were considered to be preplanned movement characteristics used by the central nervous system (CNS) to make a choice from the many possible movements that could be performed with the available degrees of freedom (Flash and Hogan 1985; Jordan et al. 1994; Morasso 1981). Other perspectives favoring central control as a source for the KIs interpret them as a result of optimization of some criterion. These may include minimization of jerk (Hogan 1984; Richardson and Flash 2002; Viviani and Flash 1995), minimization of variance caused by the inherent noise in the motor system (Harris and Wolpert 1998), or the implementation of the physical principle of least action suggesting that the CNS chooses the most economic way to execute a given path (Lebedev et al. 2001). The central origin of the KIs is supported by observations that the power law exhibits robustness under various tasks and conditions. For instance, the power law was documented with relation to isometric conditions (Massey et al. 1992), hand area motor cortical activity (Schwartz 1994), and eye movements during smooth pursuit (De'Sperati and Viviani 1997). Other studies argued that the KIs might be by-products of mechanisms not related to central control. Gribble et al. (1996) demonstrated that limb dynamics and the spring-like properties of muscles could cause a kinematic relationship (1). Todorov and Jordan (1998) inferred the power law from the smoothness of end-point trajectory. Schaal and Sternad (2001) advanced these findings by demonstrating that both trajectory smoothness, and hence, the power law can be accounted for with forward kinematic transformations of the arm and sinusoidal-like movements at the joints.

Although the proposed interpretations of the KIs are different from each other, all aforementioned studies reported a good fit of the theoretical predictions with experimental data. This makes it difficult to distinguish the true origin of the KIs among the variety of the suggested principles. This uncertainty might be partially caused by a lack of formal definitions that would allow quantification of the KIs. For instance, the bell shape of the velocity profile is under-defined because any smooth single-peaked velocity profile can be described as having this shape. Furthermore, the power law (1) is a general relationship between velocity and curvature, whereas the gain factor K and movement and/or task characteristics defining its value are unknown. To provide strict definitions of these KIs, factors that quantitatively define the KI parameters (the peak, slopes, and smoothness of the velocity profile, and the gain factor K) must be revealed. This would help to clarify factors underlying the KIs.

Although none of the previous investigations explicitly specified characteristics defining the KI parameters, Schaal and Sternad (2001) suggested a possible means for accomplishing this regarding the gain factor K. They hypothesized that the power law emerges from an approximation of arm kinematics with a linear model and an estimation of joint movements with sinusoids. A principal possibility to express K through the parameters of the arm's kinematics structure and sinusoidal joint movements is demonstrated in the appendix of that study. However, an actual expression was not obtained, probably, because three-dimensional movements were considered, which makes arm kinematics too complicated for obtaining an efficient analytical description for K. For this reason, the validation of the hypothesis was limited to an experimental demonstration that non-linearities of arm kinematics caused by increases in movement size result in larger violations of the power law. Although these arguments suggest that the non-linear arm kinematics likely contribute to the power law violations, they do not make it clear to what extent this factor defines the power law and whether other factors can also contribute to this KI. As a result, the power law origins were not fully clarified. Furthermore, the role of the arm's kinematic structure and sinusoidal joint movements was hypothesized by Schaal and Sternad (2001) only with respect to the power law. The association between these factors and the production of the two KIs related to point-to-point movements (i.e., the bell shape of the velocity profile and straightness of the trajectory) has never been considered.

The purpose of the present study is to establish explicit relationships between sinusoidal joint motions and the KIs, and thus, to clarify the role of the arm's kinematic structure and sinusoidal joint movements in emergence of the KIs. To achieve this goal, a model of arm kinematics is developed for a simplified case involving two-dimensional planar movements caused by rotations at the shoulder and elbow. Periodic sinusoidal rotations at the two joints are considered that result in cyclical motion of the end-point. This model allows examination of two types of movements that are usually considered in KI studies and that can be distinguished by relative phase between shoulder and elbow motions. The first type is characterized by a relative phase that differs from 0 and from π. These movements represent continuous drawing of curvilinear shapes, such as ellipses. They are used to examine the power law. The second type is defined by a relative phase equal to 0 or to π. Point-to-point movements have this property because during these movements, both joints usually reverse motion simultaneously. This condition for relative phase is used to address the straightness of trajectory and the shape of the velocity profile. Because cyclical movements are studied, a "dome" shape of the velocity profile will be considered instead of the "bell" shape. This is because the bell shape is usually observed during discrete movements due to zero acceleration at the initial and final positions. During cyclical movements, acceleration is not equal to zero at these extreme positions. Therefore, a dome shape is a more appropriate description of the velocity profile. In both cases, velocity has a single peak.

The simplified model of arm kinematics derived here explicitly predicts all three KIs. It also quantitatively predicts the gain factor K and the dome shape of the velocity profile and their dependence on characteristics of the arm's kinematic structure and joint rotations. Furthermore, the model also clarifies the conditions for KI violations. In addition to the three well-known KIs, kinematic regularities in end-point motion that are less recognized are predicted with the model. The majority of the predictions are obtained with the assumption that amplitudes of joint movements are small. To validate the model for regular joint amplitudes, predicted values of the KI parameters (the gain factor K, velocity peak, and trajectory straightness) are compared with those experimentally obtained during relatively large planar two-joint movements. The remarkable fit of the analytical and experimental data confirms a strong relation of the KIs to the approximation of arm kinematics with planar two-joint model and sinusoidal joint motions. These results also point to practical utility of the model, showing that it is relevant to human performance over a wide range of movements.

2 Methods

2.1 Kinematic model of the arm

A description of end-point motion depending on rotations at the arm joints is developed in this section. To facilitate analytical transformations, a simplified case of planar two-joint (shoulder and elbow) arm movements is considered, as schematically shown in Fig. 1. It is assumed that the end-point E performs cyclical motion around a center O. For instance, when circle drawing is performed, the point O is the center of the circle. When point-to-point movements are performed, the point O is the middle of the line connecting the two targets. Absolute Cartesian coordinate frame X,Y associated with the trunk position and centered at the shoulder joint S is used to describe position $[x(t), y(t)]$ of the end-point E at each moment of time t. The joint angles are denoted with γ_p and γ_d, where p and d correspond to the proximal (shoulder) and distal (elbow) joint, respectively. The angle γ_p is the angle between the upper arm and the X axis, and γ_d is the angle complementary to the

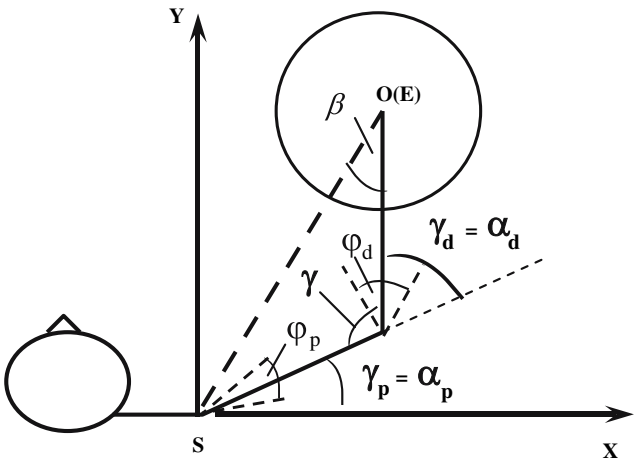

Fig. 1 Schematic representation of the arm model. The model includes shoulder and elbow movements in the horizontal plane. An orthogonal coordinate system X,Y is centered on the shoulder joint S and the direction of the axes is associated with the trunk position. Point O is a center of the working space where motion of the arm endpoint E is performed. For instance, when a *circle* is drawn, O is the circle center. Shoulder angle γ_p and elbow angle γ_d describe current position of the arm. They are equal to α_p and α_d when the end-point E is in the center O. Angles φ_p and φ_d describe deviations of the upper and lower arm from the position achieved when the hand is in the center O. The angle between the line SO and the forearm is denoted by β. Explanations for the other notations are given in the text

relative angle γ between the upper and lower arm. The assumption that cyclical movements are performed suggests that the joint angles change as

$$\begin{aligned}\gamma_p(t) &= \alpha_p + \varphi_p(t)\\ \gamma_d(t) &= \alpha_d + \varphi_d(t),\end{aligned} \tag{2}$$

where α_p, α_d are the shoulder and elbow angles when the end-point E is in the center O and $\varphi_p(t)$, $\varphi_d(t)$ are periodic functions describing joint motions as deviations from α_p and α_d. Because joint movements are usually close to sinusoids (Bernstein 1984; Buchanan et al. 1997; Schaal and Sternad 2001; Soechting and Lacquaniti 1986; Soechting and Terzuolo 1987), they can be approximated with the first term of the Fourier series, i.e., with a sinusoid of the movement frequency and amplitude

$$\begin{aligned}\varphi_p(t) &\cong A_p \sin(\omega t)\\ \varphi_d(t) &\cong A_d \sin(\omega t + \theta).\end{aligned} \tag{3}$$

Here $\omega = 2\pi f$, f is frequency of joint movements, A_p and A_d are amplitudes of the distal and proximal joint, respectively, θ is relative phase between the elbow and shoulder movements measured in radians. Finally, it is assumed that α_d is not near 0 or π (which corresponds to the physical limits for elbow rotation due to the musculoskeletal structure of the elbow joint) and that neither of A_p and A_d is trivial relative to the other (i.e., both joints are involved in motion).

Relative phase θ provides the distinction between point-to-point movements and movements involving continuous drawing of curvilinear shapes. When θ is equal to 0 or to π, the two joints simultaneously reverse motion at the extreme points of the trajectory, resulting in reversals of the end-point, and thus, in point-to-point movements. This case ($\theta = 0$ or $\theta = \pi$) will be used to consider the two KIs related to the trajectory straightness and the bell shape of the velocity profile. When there is a phase off-set between the shoulder and elbow motions, i.e., θ differs from 0 and π,curvilinear drawing movements emerge (such as ellipse drawing) because the end-point is constantly in motion. This case ($\theta \neq 0$ and $\theta \neq \pi$) will be used to study the power law.

Coordinates x and y of the arm end-point are expressed through the joint angles as

$$\begin{aligned}x &= l_p \cos(\gamma_p) + l_d \cos(\gamma_p + \gamma_d)\\ y &= l_p \sin(\gamma_p) + l_d \sin(\gamma_p + \gamma_d),\end{aligned} \tag{4}$$

where l_p, l_d are lengths of the upper and lower arm, respectively. Differentiation of (4) yields expressions for $\dot{x}, \dot{y}$

$$\begin{aligned}\dot{x} &= -l_p \sin(\gamma_p)\dot{\gamma}_p - l_d \sin(\gamma_p + \gamma_d)(\dot{\gamma}_p + \dot{\gamma}_d)\\ \dot{y} &= l_p \cos(\gamma_p)\dot{\gamma}_p + l_d \cos(\gamma_p + \gamma_d)(\dot{\gamma}_p + \dot{\gamma}_d)\end{aligned} \tag{5}$$

and for $\ddot{x}, \ddot{y}$

$$\begin{aligned}\ddot{x} &= -l_p \cos(\gamma_p)\dot{\gamma}_p^2 - l_p \sin(\gamma_p)\ddot{\gamma}_p - l_d \cos(\gamma_p + \gamma_d)\\ &\quad \times(\dot{\gamma}_p + \dot{\gamma}_d)^2 - l_d \sin(\gamma_p + \gamma_d)(\ddot{\gamma}_p + \ddot{\gamma}_d)\\ \ddot{y} &= -l_p \sin(\gamma_p)\dot{\gamma}_p^2 + l_p \cos(\gamma_p)\ddot{\gamma}_p - l_d \sin(\gamma_p + \gamma_d)\\ &\quad \times(\dot{\gamma}_p + \dot{\gamma}_d)^2 + l_d \cos(\gamma_p + \gamma_d)(\ddot{\gamma}_p + \ddot{\gamma}_d).\end{aligned} \tag{6}$$

These expressions are used in Sect. 3 to analytically derive predictions about characteristics of end-point movements during curvilinear-drawing tasks ($\theta \neq 0$ and $\theta \neq \pi$) and point-to-point tasks ($\theta = 0$ or $\theta = \pi$), and to demonstrate that the KIs are inherent features of the model kinematics. Also, the following formula for curvature C of end-point trajectory will be used

$$C = \frac{\begin{vmatrix}\dot{x} & \dot{y}\\ \ddot{x} & \ddot{y}\end{vmatrix}}{(\dot{x}^2 + \dot{y}^2)^{3/2}} = \frac{|\dot{x}\ddot{y} - \ddot{x}\dot{y}|}{V^3}. \tag{7}$$

In addition to analytical conclusions, Sect. 3 includes a demonstration of the validity of the theoretical predictions with use of experimental data. The experimental methods are described next.

2.2 Experimental design and procedure

Cyclical drawing of ovals and straight lines was performed in the experiment. The oval drawing data are used here to verify analytical predictions with respect to the power law. The line-drawing tasks are utilized to validate predictions for the two KIs related to point-to-point movements. Line-drawing movements are a specific case of point-to-point movements (i.e., movements during which $\theta = 0$ or $\theta = \pi$) that include an additional constraint of a straight trajectory. The line drawing data are used here to investigate whether there were movements during which straightness of trajectory decreased in spite of the explicit requirement to move along a straight line, and whether these decreases were associated with deviations of joint motions from sinusoids and/or with deviations of θ from 0, π. The line-drawing data are also used to test quantitative predictions with respect to end-point velocity.

The experiment used in the present study is described in detail in previous publications (Dounskaia et al. 2002a,b). Therefore, only a brief description is provided here. Arm motion during cyclical drawing of elliptical shapes and straight lines was recorded. Ten

right-handed subjects were recruited from the Arizona State University campus to participate. All volunteers received a brief explanation of the experiment, and they signed an informed consent in accordance with policies of the Human Subjects Institutional Review Board of Arizona State University. Subjects moved the tip of the index finger along templates presented on a horizontal table in front of them. The templates were a circle of 18 cm diameter, four ellipses with principal diameters of 25 and 12.5 cm, and four lines with length of 30 cm. The ellipses and lines were oriented in different directions: anterior–posterior (" *vertical*"), lateral (" *horizontal*"), *tilted right*, and *tilted left*. The templates had a common center. Location of the center was individually adjusted to the position of the fingertip when the shoulder angle α_p was $\pi/9$ (20°) and the elbow angle α_d was $\pi/2$ (90°).

According to the requirements of the model, movements were planar and performed by the shoulder and elbow. Arm motion was performed in the horizontal plane by adjusting the height of the table for each subject. Motion was restricted to rotations at the shoulder and elbow, and the trunk and wrist were immobilized. Two levels of cyclic frequency guided by a metronome were used, 1.0 and 1.5 Hz. Each trial lasted for 12 s. Joint and end-point movements were registered with use of an OPTOTRAK 3D optoelectronic camera system. Infrared light emitting diodes were placed on the trunk (sternum), shoulder, elbow, and index fingernail of the right arm. The OPTOTRAK data were filtered with 15 Hz cut-off low-pass Butterworth digital filter and then used to compute joint movement characteristics, such as frequency, amplitude, and relative phase as described by Dounskaia et al. (2002a). The data from the diode on the fingertip were used to compute characteristics of the arm end-point motion. End-point velocity was calculated as $V = \sqrt{\dot{x}^2 + \dot{y}^2}$ and curvature of the trajectory was computed with (7), where x and y are coordinates of the fingertip diode in the horizontal plane. Lengths of the arm segments were determined for each subject as $l_p = 0.18H$ and $l_d = l_f + l_h = 0.146H + 0.098H = 0.244H$, where l_f and l_h are the lengths of the forearm and hand, respectively, and H is the body height (Chaffin and Andersson 1984).

3 Results

3.1 Analytical predictions for characteristics of end-point movements

The KIs are analytically derived in this section for two types of movements: curvilinear trajectories of the end-point (such as a circle or an oval) that emerge when relative phase θ between the shoulder and elbow movements differs from 0 and π, and point-to-point movements that require θ to be equal to 0 or π.

3.1.1 *The power law while drawing curvilinear shapes ($\theta \neq 0$ and $\theta \neq \pi$)*

This KI can be derived from expression (7) for line curvature C. When the sign of curvature is ignored and curvature is always positive, this expression yields

$$V = \frac{(|\dot{x}\ddot{y} - \ddot{x}\dot{y}|)^{1/3}}{C^{1/3}}. \tag{8}$$

Comparison of (8) with (1) indicates that K is defined as

$$K = (|\dot{x}\ddot{y} - \ddot{x}\dot{y}|)^{1/3}. \tag{9}$$

It is shown in Appendix A that K defined by (9) varies during movement and that the variations decrease and K approaches a constant when joint amplitudes A_p, A_d decrease. This result was obtained by Schaal and Sternad (2001) with consideration of linear approximations of arm kinematics. However, an expression for the constant that estimates K was not obtained. Due to the simplicity of the present model, an explicit estimation of K through the kinematic parameters can be derived. As shown in Appendix A, the following prediction can be formulated

Prediction 1 The gain factor K in (1) can be approximated by

$$K^* = \omega\left[l_p l_d A_p A_d \sin(\alpha_d) \sin(\theta)\right]^{1/3}. \tag{10}$$

Note that although K can deviate from the constant K^* predicted by (10) when joint amplitudes are not small, this deviation is limited due to the properties of the function $f(z) = z^{1/3}$ in (9). The value of $f(z)$ changes slowly in comparison with changes in the argument z for all values of z that are not very small (approximately, higher than 1.0), as shown in Fig. 2. This property can be illustrated with an example of circle drawing with average joint movement parameters converted in degrees $A_p = 26.5°, A_d = 35.9°, \theta = 135°$ documented in our previous study (Dounskaia et al. 2002a). With the use of 1.5 Hz cyclic frequency and of arm segment lengths $l_p = 0.30$ m and $l_d = 0.41$ m calculated as described in Sect. 2 for body height $H = 1.7$ m, (10) results in an estimation $K^* = 1.74$. Computed from (9) in assumption that joint movements were sinusoidal, K is a periodic function of time that varies between 1.58 and 1.88. However, the argument $z = |\dot{x}\ddot{y} - \ddot{x}\dot{y}|$ of the 1/3-power function in (9) varies between 3.88 and 6.65. This example demonstrates that z can vary substantially during

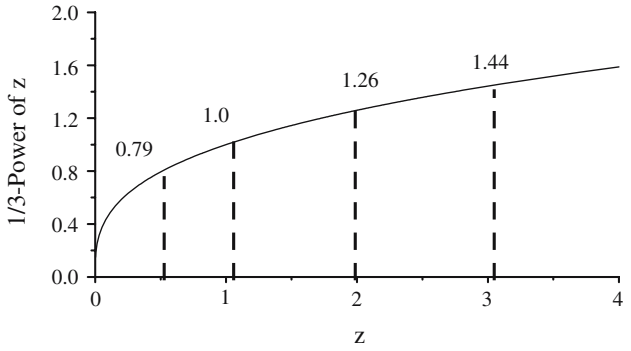

Fig. 2 The plot of the function $f(z) = z^{1/3}$ demonstrates that the 1/3-power function rapidly increases when the argument has small values. However, when the argument is higher than 1.0, the function changes slowly. For instance, $f(z) = 1.0$ for $z = 1.0$ and $f(z) = 1.44$ when $z = 3$

arm movements. However, if values of z remain sufficiently high, K might be relatively constant due to the properties of the 1/3-power function in (9). Note that (9) does not include the limitations of the derived kinematic model. The model only allowed the assessment of the argument z for the example of a typical arm movement. This suggests that power law (1) holds (approximately) during any movement that results in sufficiently high value of z. In other words, *the power law follows from the definition (7) of curvature C when the argument of the 1/3-power function in (9) is sufficiently high* (approximately, higher than 1.0). The above numerical example and the experimental data reported in Sect. 3.2 suggest that typical arm movements performed with sinusoidal-like joint motions satisfy this condition. Figure 2 also shows that when z is small, relative variability of K is high. However, absolute variability might be still small because K is small.

The model allows further clarification of conditions underlying the constancy of K by specifying the dependence of K on kinematic parameters. Expression (10) shows that K depends on motion frequency ω, lengths of the upper and lower arm l_p and l_d, amplitudes A_p and A_d of the shoulder and elbow motion, relative phase θ, and the elbow angle α_d achieved when the arm endpoint is located in the center of the working space. This expression also reveals conditions for violation of the power law (i.e., conditions for variability of K) during movements described by the model. Appendix A shows that variability of K might increase, first, in conditions that make the argument z of the 1/3-power function in (9) highly variable. These conditions include high joint amplitudes, and specifically, large range of elbow motion that makes the approximation of the elbow angle with constant α_d invalid. Second, conditions that make the argument z small can result in significant variability of K. For instance, K can vary dramatically when θ is close to 0° or to π and when movement is performed with the elbow position close to extreme flexion or extension ($\alpha_d = 0$ or $\alpha_d = \pi$). Furthermore, the argument z can be small when joint amplitudes are small. Thus, both high and low amplitudes can cause increases in K variability. High amplitudes can cause this effect because they increase the variability of z. Low amplitudes can bring this argument in the region where the 1/3-power function changes fast. This complex dependence of K on joint amplitudes differs from that predicted by Schaal and Sternad (2001), as considered in more detail in Sect. 4.

Expression (10) was obtained with the assumption that movements at the shoulder and elbow have the same frequency. Lebedev et al. (2001) analytically demonstrated that if movement frequencies at the two joints are different, K is not constant but changes as a function of time and hence the power law does not hold. This can also be shown with use of the present model. It can be demonstrated that if φ_p and φ_d in (3) have different frequencies, K cannot be approximated with a constant.

3.1.2 Straightness of trajectory during point-to-point movements ($\theta = 0$ or $\theta = \pi$)

It is demonstrated in this subsection that this KI is predicted by the model when $\theta = 0$ or $\theta = \pi$ and A_p, A_d are small. This can be shown by considering the representation of trajectory curvature that follows from (7)

$$C = K^3 \Big/ V^3. \tag{11}$$

It is shown in Appendix A that $K^3 = F_1 + F_2$. Formula (A2) in Appendix A also shows that $F_1 \equiv 0$ when $\theta = 0$ or $\theta = \pi$, and hence, $C = (F_2/V)^3$. Since F_2 depends on the third power of A_p and A_d (see A2 in Appendix A) and V depends only on the first power of joint amplitudes [as observed from (13) derived further], F_2 decreases faster than V, and therefore, C approaches zero when joint amplitudes decrease. This justifies

Prediction 2 Cyclical point-to-point movements performed with sinusoidal joint motions of small amplitude will have nearly straight trajectories.

This prediction implies that decreases in trajectory straightness might be caused by deviations of joint motions from sinusoids. Supportive experimental evidence is presented in Sect. 3.2. Another possible reason for curved trajectory is high joint amplitudes. This prediction is in agreement with data reported by Haggard and Richardson (1996) and by Pollick and Ishimura (1996).

3.1.3 Dome-shaped velocity profile during point-to-point movements ($\theta = 0$ or $\theta = \pi$)

This KI can be demonstrated by calculation of the end-point tangential velocity as $V = \sqrt{\dot{x}^2 + \dot{y}^2}$ with use of (5), which results in

$$V^2 = l_p^2\dot{\varphi}_p^2 + l_d^2\left(\dot{\varphi}_p + \dot{\varphi}_d\right)^2 + 2l_p l_d \cos\left(\alpha_d + \varphi_d\right)\left(\dot{\varphi}_p + \dot{\varphi}_d\right). \tag{12}$$

When sinusoidal approximations (3) of joint movements with $\theta = 0$ and $\theta = \pi$ are used, (12) becomes

$$V = \omega|\cos(\omega t)|\sqrt{L^2A_p^2 + l_d^2A_d^2 \pm A_dA_p\left(L^2 + l_d^2 - l_p^2\right)}, \tag{13}$$

where L is the distance between the shoulder joint S and the end-point E, "+" under the radical stands for $\theta = 0$ and "−" stands for $\theta = \pi$. The function $|\cos(\omega t)|$ has a dome shape because it is equal to zero at the extreme points of the trajectory and it has a single maximum at the midpoint. Changes in L are limited and monotonic within each stroke (half cycle). Therefore, V has a single peak, or in other words, it has a dome-shaped profile. These considerations result in

Prediction 3 During cyclical point-to-point movements performed with sinusoidal joint motions, each stroke will have dome-shaped velocity V defined by (13) with a peak value assessed by

$$V_{\text{peak}} = \omega\sqrt{L^2A_d^2 + l_p^2A_p^2 \pm A_dA_p\left(L^2 + l_d^2 - l_p^2\right)}, \tag{14}$$

where L is the distance between the shoulder position S and the midpoint O of the trajectory.

In contrast to representations (10) and (11), estimations (13) and (14) are valid when joint amplitudes are not small. This suggests that the dome shape of the velocity profile is a more robust KI as compared to the other two KIs.

The above analytical considerations provide interpretation for the three well-known kinematic invariants for the case of cyclical movements: the power law while drawing curvilinear shapes, and the straight trajectory and single-peaked velocity profile during point-to-point movements. Next, the derived model is used to make explicit two other invariants of end-point kinematics that are useful for human movement research. These invariants are related to the influence of joint coordination patterns on the velocity and distance of the end-point movement.

3.1.4 Dependence of peak velocity on shoulder and elbow coordination pattern during point-to-point movements ($\theta = 0$ or $\theta = \pi$)

There are only two possible shoulder and elbow coordination patterns during point-to-point movements. The two joints either flex and extend simultaneously ($\theta = 0$) or flexion at one joint is accompanied by extension at the other joint ($\theta = \pi$). The dependence of the sign under the radical in (13) and (14) on the joint coordination pattern suggests

Consequence 1 During movements for the same distance, end-point peak velocity is higher when $\theta = 0$ than when $\theta = \pi$ if characteristics of joint movements are the same.

This prediction is supported in Appendix B and illustrated in Fig. 3. In this figure, $\mathbf{V}_{\text{sf}}$ is the endpoint velocity component produced by shoulder flexion. This vector is orthogonal to SO. $\mathbf{V}_{\text{ef}}$ and $\mathbf{V}_{\text{ee}}$ are the velocity components produced by elbow flexion and extension, respectively. The figure shows that if $|\mathbf{V}_{\text{ef}}| = |\mathbf{V}_{\text{ee}}|$, the end-point velocity is higher when the two joints rotate in-phase (resulting in $\mathbf{V}_2$) than when they rotate anti-phase (resulting in $\mathbf{V}_1$) due to the kinematic structure of the arm.

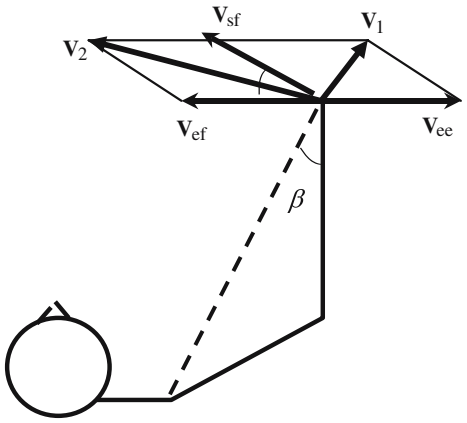

Fig. 3 Dependence of arm endpoint velocity on joint coordination pattern. A vector of arm endpoint velocity emerges as a sum of two vectors caused by rotations at the shoulder (this vector is orthogonal to SO) and elbow (this vector is orthogonal to the forearm), respectively. When the shoulder flexes and the elbow extends, the endpoint velocity is described by vector $\mathbf{V}_1$ that is equal to a sum of $\mathbf{V}_{\text{sf}}$ and $\mathbf{V}_{\text{ee}}$. When both the shoulder and elbow flex, the endpoint velocity is a sum of $\mathbf{V}_{\text{sf}}$ and $\mathbf{V}_{\text{ef}}$ and is the vector $\mathbf{V}_2$. If $|\mathbf{V}_{\text{ef}}| = |\mathbf{V}_{\text{ee}}|$, the resultant velocity is higher when both joints flex than when one joint flexes and the other extends

Table 1 Mean and SD of movement characteristics

Templates									
Elbow amplitude	35.9°	47.6°	27.4°	38.2°	31.9°	59.0°	11.7°	49.5°	41.4°
SD	1.7°	1.8°	1.6°	1.9°	2.0°	2.4°	3.6°	1.8°	4.1°
Shoulder amplitude	29.7°	32.7°	29.8°	22.7°	38.1°	32.3°	33.1°	6.7°	43.3°
SD	2.5°	2.8°	2.5°	2.4°	2.2°	3.3°	3.4°	1.8°	5.0°
Relative phase	140°	158°	120°	113°	148°	181°	47°	239°	181°
SD	14.6°	15.9°	17.8°	8.6°	17.3°	2.1°	48.8°	82.3°	1.7°
Elbow power portion	0.89	0.91	0.88	0.9	0.89	0.91	0.50	0.79	0.85
SD	0.04	0.04	0.05	0.04	0.04	0.04	0.25	0.12	0.13
Should. power portion	0.90	0.89	0.89	0.89	0.90	0.90	0.92	0.47	0.87
SD	0.04	0.10	0.06	0.04	0.06	0.04	0.04	0.25	0.10
Mean of β	38.3°	38.8°	36.6°	37.2°	38.3°	39.1°	35.7°	37.5°	38.0°
SD	4.6°	4.6°	4.6°	4.5°	4.2°	4.3°	4.5°	4.6°	3.7°
Range of β	11.0°	14.5°	8.7°	11.7°	9.9°	17.5°	3.2°	14.5°	12.2°
SD	2.3°	3.5°	2.1°	2.8°	2.0°	4.1°	1.3°	4.3°	2.1°

Angular values are given in degrees

3.1.5 Distance of point-to-point movements ($\theta = 0$ or $\theta = \pi$).

Another consequence of (13) can be formulated as

Consequence 2 Movement distance D of the arm end-point is shorter during the in-phase ($\theta = 0$) than during anti-phase ($\theta = \pi$) joint coordination pattern if joint movement amplitudes are the same.

Support for Consequence 2 for the case of small joint amplitudes is provided in Appendix C. The dependence of end-point motion characteristics on joint coordination patterns addressed by these two predictions is important when arm movements in different directions are studied (Hogan 1985; Graham et al. 2003).

The formulated predictions have been derived in assumption of sinusoidal joint motions. Further, small joint amplitudes were assumed for the majority of these predictions. The extent to which these predictions are violated during natural arm movements needs to be investigated experimentally. The next section addresses the experimental validation of Predictions 1, 2, and 3. It is demonstrated that the three predictions are relevant for relatively large movements and that expressions (10) and (14) accurately assess K and the velocity peak. The reported results show that the model is valid for human movements over a range of typical behaviors, and that the three KIs are related to the arm kinematics structure and sinusoidal joint motions.

3.2 Experimental support

Characteristics of joint movements averaged across the two frequency levels and across subjects are shown in Table 1. Drawing the nine shapes required various combinations of elbow and shoulder movements, as observed from the variations in shoulder and elbow amplitude and relative phase shown in the top six rows of Table 1. The next four rows in this table represent the power portion, a characteristic used to verify whether joint movements were close to sinusoids. The power portion is an assessment of relative power attributed to the movement frequency component obtained with the FFT analysis. To compute power portion, first, a power spectrum for each joint displacement profile was calculated with use of the FFT analysis. Then a ratio was calculated between the total power (that was estimated with a sum of power spectrum values up to 10 Hz frequency) and the power of the registered movement frequency in the interval between +0.2 and −0.2 Hz. This ratio is representative of a portion of the power related to the movement frequency component. When joint excursion has a perfect sinusoidal profile, this portion would be equal to 1.0. Deviations of joint excursion from a sinusoid are characterized by decreases in the power portion. Next these and other results are considered separately for the oval and circle drawing and for the line drawing.

3.2.1 Oval and circle drawing

As it was expected, relative phase differed from 0 and from π for all five curvilinear shapes. The power portions were close to 0.9 for all these shapes both at the shoulder and elbow. Concentration of power in a small portion of the frequency range suggests that joint movements were close to sinusoids.

The experimental data were utilized to test Prediction 1 that the gain factor K in (1) can be assessed with (10) as a function of a number of movement parameters ($\omega, l_p, l_d, A_p, A_d, \theta,$ anda_d). The average K values computed for each trial with (10) and with (1) were

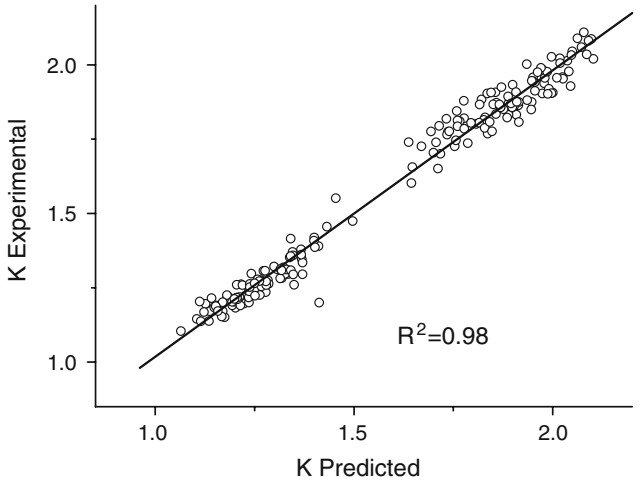

Fig. 4 The experimentally obtained values of the gain factor K (*y-axis*) plotted against K values predicted by the model (*x-axis*) during circle and oval drawing. The experimental values were computed directly from fingertip motion with use of empirical relationship (1). The predicted values were computed with (10) from individual arm segment lengths and characteristics of joint movements. Each data point represents a single movement trial. The *regression line* and the high R^2 value demonstrate that the model accurately predicted the experimental data

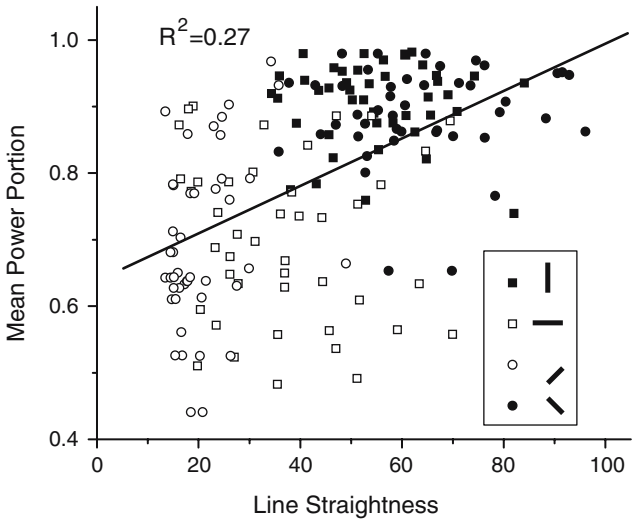

Fig. 5 Mean power portion for the shoulder and elbow plotted against trajectory straightness. The *data points* correspond to individual trials performed at the two frequency levels. The *data* are denoted by four different symbols corresponding to the four line orientations. The *regression line* was computed for the data obtained for all four line orientations. In spite of the requirement to draw straight lines, trajectory straightness varied. Decreases in straightness were associated with lower sinusoidality of joint motions

compared with each other. The calculations prescribed by (10) were performed with the use of segment lengths and mean values of frequency, amplitude, and relative phase of joint movements calculated for each trial. The experimental data of the end-point velocity and curvature were used to compute K with (1). The experimental values of K plotted against the data predicted by (10) are shown in Fig. 4 together with results of a linear regression analysis. The slope of the regression line was close to 1.0 ($b = 0.96$), the intercept was close to 0.0 ($a = 0.05$), and the R^2-value was high ($R^2 = 0.98$). These regression parameters demonstrate that the two data sets were remarkably similar. This similarity confirms the validity of the K estimate given by (10). It also shows that Prediction 1 can be valid for substantial joint amplitudes, and not only for small joint amplitudes for which this prediction was derived.

3.2.2 Line drawing

The requirement for these movements was to slide the fingertip along a line template back and forth between the two ends of the line. In other words, subjects were required to perform point-to-point movements with straight trajectory. This task potentially allows verification of Predictions 2 and 3. Any deviation of the trajectory from straightness or lack of dome shape in the velocity profile should be associated with non-sinusoidality of joint motions and/or deviation of θ from $0, \pi$. If the velocity profile is dome shaped, then the peak velocity should be predicted by (14).

Figure 5 demonstrates the relationship between trajectory straightness and sinusoidality of joint motions. Trajectory straightness was computed as a ratio between the length of the line connecting the two extreme points in each stroke and the maximal deviation of the actual trajectory from this line. Thus, increases in this characteristic correspond to improvements in trajectory straightness. The vertical axis shows power portion averaged for the shoulder and elbow. Obviously, decreases in trajectory straightness were accompanied with decreases in joint motion sinusoidality. However, the relatively low correlation coefficient ($R = 0.52$) shows that the sinusoidality was not the only factor associated with decreases in trajectory straightness. In particular, less straight movements were characterized by deviations of θ from $0, \pi$. This can be inferred from an observation that trajectory straightness was lower for the lines that were characterized by θ different from $0, \pi$. Figure 5 shows that trajectory was straighter while drawing of the vertical and left-tilted lines than of the horizontal and right-tilted lines. This observation was confirmed by a 4×2 (Line $\times$ Frequency) ANOVA with repeated measures applied to the straightness data. The main effect of the line factor was significant [$F(3, 30) = 39.6$, $P < 0.001$]. Post hoc testing specified that straightness was similar for the vertical and left-tilted line and it was

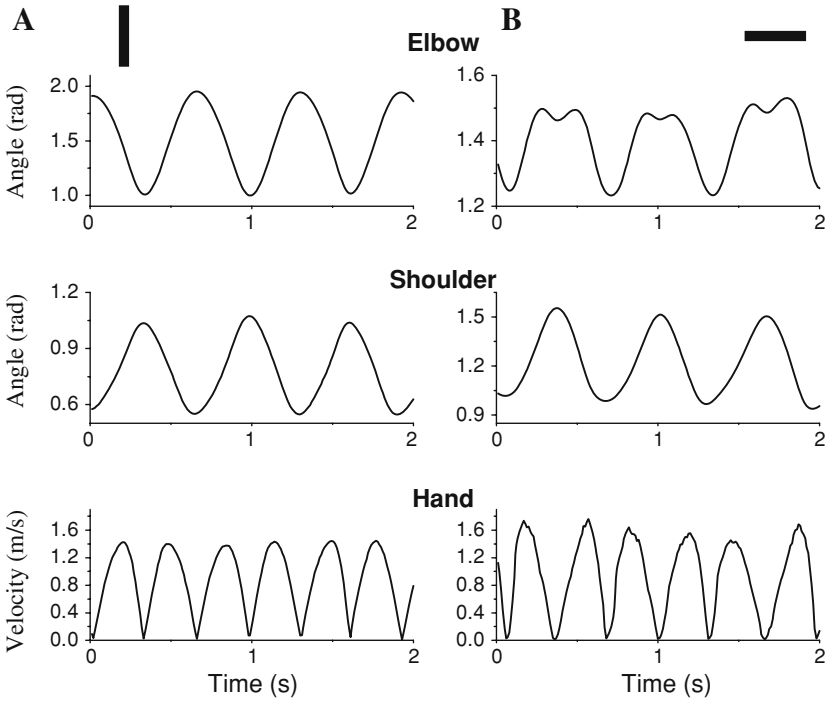

Fig. 6 Individual data obtained during drawing the vertical line (*left column*) and the horizontal line. The *top and medium panels* show angular displacements at the joints and the *bottom panels* demonstrate endpoint velocity. During drawing the vertical line, movements at both joints were sinusoidal-like and the hand velocity was smooth and had a single peak within each cycle. During drawing the horizontal line, elbow angular displacement had more than single peak within each cycle. This was accompanied by distortions of the bell shape in the endpoint velocity profile

higher for these lines than for the other two lines. Furthermore, straightness was higher for the horizontal than for the right-tilted line. The main effect of frequency was also significant [$F(1,10) = 8.5$, $P < 0.05$]. Straightness decreased with increases in frequency level, specifically for the horizontal and for the right-tilted line. However, the interaction did not reach significance ($P = 0.08$).

The differences in the trajectory straightness across the lines suggest that straightness decreased when θ deviated from 0, π. Indeed, the data in Table 1 show that while drawing the vertical and left-tilted line, relative phase θ was close to π. An example of joint motions while drawing the vertical line at 1.5 Hz frequency is given in the left column of Fig. 6a. The joint displacements were coordinated with $\theta \approx \tilde{\pi}$ and they were close to sinusoidal with power portion equal to 0.89 and 0.93 at the shoulder and elbow, respectively. Relative phase differed from the expected values while drawing the horizontal and right-tilted line. The high SD suggests that relative phase was not consistent and varied in a wide range for these two lines. The reason for this is that mean relative phase presented in Table 1 was computed as an average of continuous relative phase during the entire movement instead of only at the discrete reversal points. Only one joint performed a sinusoidal movement, whereas motion at the other joint had short amplitude and was irregular during the drawing of these two lines. This caused variations in relative phase during each movement stroke, resulting in a variable mean relative phase. The joint amplitude and power portion data in Table 1 confirm this statement, showing that drawing the line tilted right was predominantly performed by the elbow with an irregular motion of low amplitude at the shoulder. While drawing the horizontal line, shoulder motion was close to a sinusoid but elbow motion, on average, was not sinusoidal. Visual inspection revealed that elbow angular velocity often had two peaks within each movement stroke. An example of a movement having a two-peak angular velocity at the elbow is shown in Fig. 6b. For this movement, power portion was 0.90 at the shoulder and 0.55 at the elbow and mean θ was 0.76 (43.6°).

These results support Prediction 2, showing that in spite of the explicit requirement to move along a linear template, trajectory straightness varied across the lines. In general, lower straightness was associated with lower sinusoidality of joint motions and deviations of θ from $0, \pi$. Further, these results suggest validity of Prediction 2 for substantial amplitudes of joint motions and not only for small amplitudes included in the formulation of this prediction. Thus, straightness of trajectory often observed during point-to-point movements might be in many cases a mere consequence of sinusoidal-like joint motions.

The data also supported Prediction 3 with respect to the dome shape of the velocity profile whose peak is predicted by (14). In agreement with this prediction, velocity profile usually had smooth and symmetrical dome shape while drawing the vertical and left-tilted line (when both joint motions were close to sinusoids), and this shape was often distorted while drawing the horizontal and right-tilted line (when motion at one joint

was not sinusoidal). This is illustrated in Fig. 6 where the bottom panels show two examples of velocity profiles obtained for the vertical and horizontal line.

According to the prediction of the model, the dome shape emerges due to the cosine function in (13). To examine whether velocity profile was close to this shape, power portion was computed for signed end-point velocity. The sign changed depending on the direction of movement along the line template, which resulted in a periodic bi-phasic velocity profile. Mean power portion computed for these velocity profiles was 0.94 (SD = 0.03) for the vertical line and 0.93 (SD = 0.04) for the tilted-left line and it was 0.9 (SD = 0.03) and 0.88 (SD = 0.06) for the horizontal and right-tilted line, respectively. A 4 × 2 (Line × Frequency) ANOVA with repeated measures revealed significant effect of line [$F(3, 30) = 7.8$, $P < 0.01$]. Post hoc testing showed that power portion was higher for the vertical and left tilted lines than for the horizontal and right-tilted lines. The effect of frequency was not significant ($P = 0.4$).

To verify that peak velocity is predicted by (14), peak velocity was computed from (14) for each trial with the use of individual segment lengths l_p, l_d; mean joint amplitudes; and distance L from the shoulder position to the middle of the line path. These data and the peak velocity values registered by the fingernail marker were regressed against each other. Figure 7 shows the results of the regression analysis. The regression was characterized by $b = 0.84$, $a = 0.25$, and $R^2 = 0.9$, where b is the slope and a is the intercept of the regression line. Although the non-zero intercept shows that the predicted values were slightly lower than the experimental data, overall the results of the regression analysis confirm the validity of (14) for the tested movements. The good fit between the experimental and predicted values obtained even though joint motions were not always sinusoidal and there was an additional constraint to move along a straight line suggests that estimation (14) is robust and might be applicable for a wide range of point-to-point movements.

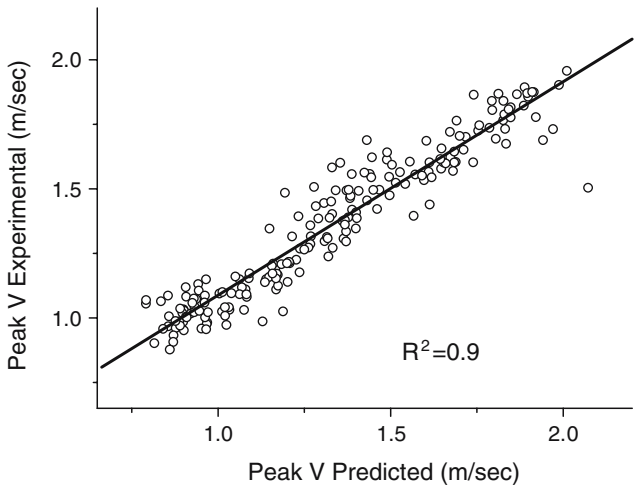

Fig. 7 Experimentally obtained peak velocity of the arm end-point (*y-axis*) plotted against peak velocity values predicted by the model (*x-axis*) during drawing the four lines. The experimental values were computed directly from fingertip motion. The predicted values were computed with (14) from individual arm segment lengths and characteristics of joint movements obtained for each trial. Each data point represents a single movement trial. The *regression line* and the high R^2 value demonstrate that the model accurately predicted the experimental data

Since movement frequency and distance were the same for all four lines, a direct verification of Consequences 1 and 2 is not possible based on the present experimental data. However, the results for joint amplitudes provide an indirect support for Consequences 1 and 2. These data show that the sum of the joint amplitudes was 42.7° while drawing the horizontal line (which required simultaneous flexion and extension at the shoulder and elbow, i.e. the in-phase coordination pattern) and it was 89.1 and 83.4° while drawing the vertical and left-tilted line, respectively (which required combination of flexion and extension at the two joints, i.e. the anti-phase coordination pattern). Drawing the right-tilted line is not included in this analysis, because it predominantly was a single-joint movement. Thus, movement of the end-point for the same spatial distance required twice shorter total angular distance at the two joints during the in-phase than during the anti-phase coordination pattern. This suggests that if amplitude of each joint was the same in the two coordination patterns and equal cyclic frequency was maintained, end-point movement distance would be longer and velocity would be higher during the in-phase pattern, as formulated in Consequences 1 and 2.

The considerations in Appendix B underlying Consequence 1 were based on the statement that the angle β is always acute during arm movements. This statement was supported by the experimental data. As shown in the four bottom rows of Table 1, mean values of β were similar across the shapes, which is consistent with the common center of the shapes. Mean value of β computed for all nine shapes was 40.2° and the mean range of β was 11.6°.

4 Discussion

Linear approximation of the arm kinematics structure when joint movements are sinusoidal has been proposed as a source of the constant gain factor K in the power law (Schaal and Sternad 2001). However, this interpretation

of the power law has not received stronger support than other interpretations because an explicit expression for K that would allow comparison of the analytically predicted K values with values obtained experimentally had not been derived. The simplification of the arm model by using planar two-degree-of-freedom movements in the present study made it possible to obtain an analytical expression for K from the definition of trajectory curvature C. This expression allowed reconstruction of full picture, revealing all factors that influence K. In particular, this expression showed that although K is a time-varying characteristic, its variability is limited due to the properties of the 1/3-power function included in the expression for K. This expression also demonstrates that in addition to increases in joint amplitudes distinguished by Schaal and Sternad (2001) as factors underlying variability in K, decreases in joint amplitude might also cause increases in K variability due to functional properties of K. The revealed complex dependence of K variability on joint amplitudes and other kinematic parameters suggests that the power law (i.e., constancy of K) holds when the shoulder and elbow perform smooth (sinusoidal-like) joint motions of moderate amplitudes with substantial phase off-set ($\theta \neq 0$ and $\theta \neq \pi$), and movements are performed in the medium portion of the arm working space (the elbow angle is not close to 0 or π).

In addition to the prediction of conditions for the power law, the model has demonstrated that the arm's kinematic structure and sinusoidal joint movements also predict the two KIs characterizing cyclical point-to-point movements, i.e., the straightness of the end-point trajectory and the dome shape of the velocity profile. It was shown that the approximation of end-point trajectory with a straight line naturally emerges when shoulder and elbow amplitudes are relatively small, and that the dome shape of the velocity profile is an inherent property of sinusoidal joint motions even when amplitudes of these motions are not small. Thus, the model revealed that all three KIs might be related to a single phenomenon, which is a novel finding that has not been proposed previously.

Another important novelty of the present study is that the derived analytical descriptions clarify definition and provide quantification of the two KIs, the power law and the dome shape of the velocity profile. Previous studies formulated the power law as a linear dependence between V and C^{ν} with the power $\nu \approx 1/3$ and a nearly constant gain factor K. Expression (9) specifies that $\nu = 1/3$ and K is a time-varying characteristic, whereas expression (10) defines the constant estimation of K and kinematic parameters determining it. Furthermore, it has been recognized in previous studies that the velocity profile during point-to-point movements is usually smooth, has a single peak, and is nearly symmetrical. The bell and dome shapes were used to describe this profile during discrete and cyclical movements, respectively. Expression (13) specifies that during cyclical movements, the velocity profile is an unsigned cosine function whose peak can be estimated with (14) from parameters of the arm structure and joint motions. The obtained quantification of the two KIs creates a mechanism for numerical and experimentally verifiable predictions of the end-point trajectory characteristics as well as for quantitative comparison of these characteristics across different movement conditions and subject groups.

The expressions predicting the KIs were derived with the assumption of small amplitudes of joint movements. However, many studies that experimentally documented the KIs were not limited to small joint amplitudes. To test the validity of the analytical predictions for joint amplitudes that are not small, the predictions were tested with use of experimental data collected while drawing a set of relatively large circular, oval, and linear shapes. The predictions related to the power law and the dome shape of the velocity profile were confirmed by comparison between the experimental data and the data computed with (10) and (14). The good fit maintained between the two data sets for various anthropometrical and kinematic parameters justifies applicability of the corresponding predictions to natural arm movements. Expression (13) defining the dome shape of the velocity profile was further validated by documenting deviations of end-point velocity from the cosine shape when motion at one joint was not sinusoidal (Fig. 6). The prediction that in-phase and anti-phase sinusoidal motions at the shoulder and elbow result in straight trajectory was supported by the finding that trajectory straightness varied across the lines in spite of the explicit requirement to move along a straight-line template, and that the decreases in straightness were associated with deviations of joint motions from sinusoids and of relative phase from 0, π. Overall, these results argue for validity of the derived model for a wide range of arm movements and confirm the relation of the three KIs to the kinematic structure of the arm and sinusoidal-like joint motions. Particularly, they show that K and peak velocity can often be accurately predicted by (10) and (14).

In addition to the three major KIs, two other regularities in end-point kinematics (Consequences 1 and 2) were deducted from the arm model. They predict that for the same shoulder and elbow amplitudes, distance and velocity of the end-point movement will be higher during the in-phase than the anti-phase joint

coordination pattern. Indirect support for these predictions was provided with shorter joint amplitudes during the in-phase coordination pattern than during the anti-phase pattern when end-point movement distance was the same. The dependence of end-point kinematics on joint coordination addressed in Consequences 1 and 2 is important when joint control is compared across different movement directions (Graham et al. 2003; Hogan 1985).

The finding that the KIs depend on kinematic parameters, such as arm segment lengths, joint movement parameters, and others, has implications for some previous experimental observations and can be useful for future research. For instance, the dependence on A_p and A_d suggests that K can vary with changes in the size of the shape. Evidence relevant to this prediction has been provided by a number of studies (Lacquaniti et al. 1983; Schaal and Sternad 2001; Sternad and Schaal 1999; Viviani and Cenzato 1985). The dependence on θ predicts that K can vary within shapes that require variable phase off-set θ. This might be one of the reasons for variations in K observed during handwriting and drawing movements and described as movement segmentation (Lacquaniti et al. 1983; Sternad and Schaal 1999; Viviani and Cenzato 1985; Viviani and Terzuolo 1982). The dependence on l_d and l_p suggests that drawing the same shape by subjects with different length of the arm segments would result in different K. Namely, K would be higher when arm segments are longer. This prediction is in agreement with the observation of age-dependent differences in K during drawing movements performed by children between 5 and 12 years of age (Viviani and Schneider 1991). In this study, K in general increased with increased age even though the value used for approximation of the curvature power was lower than 1/3 for younger children, which caused overestimation of K.

While some evidence for the dependence of K on the aforementioned parameters has been reported in previous studies, and this dependence could also be deduced from the representation of K given in the appendix by Schaal and Sternad (2001), the dependence of K on $\sin(\alpha_d)$ established by (10) has not been discussed. Nevertheless, this dependence suggests that K depends on the average arm posture during motion. For instance, K may vary across shapes whose locations require different elbow angles. In particular, differences in K are expected when the same shape is drawn with the stretched or flexed arm (α_d is close to 0 or to π, and hence $\sin(\alpha_d)$ is close to 0.0) as compared to drawing the shape with α_d close to $\pi/2$ where $\sin(\alpha_d)$ is close to 1.0. Further, the dependence on $\sin(\alpha_d)$ suggests that K may significantly vary within a shape produced with a stretched or flexed arm (α_d is close to 0 or to π) because $\sin(\alpha_d)$ is small and highly variable in these arm positions, making K highly variable due to the properties of the 1/3-power function in (9) that rapidly changes for small values of the argument (Fig. 2). For the same reason, K can be highly variable when narrow ellipses are drawn (θ is close to 0 or to π in this case, and hence, $\sin(\theta)$ is small and highly variable).

While the comparisons with the experimental data suggest that the relation between the KIs and kinematic parameters is maintained over a wide range of arm movements, the derived model has a number of limitations. First, the present study was limited to cyclical movements, and therefore, the findings do not account for some features of discrete movements, such as the asymmetric velocity profile during pointing and the dependence of velocity on the target size (Fitts 1954). It is possible that expression (13) is applicable to discrete pointing movements when the target is large, because a number of studies reported that kinematic characteristics of discrete and cyclical movements are similar for large targets, and the differences emerge when the target size is decreased (Adam et al. 1993; Buchanan et al. 2004, 2003; Guiard 1993, 1997). Additional research is necessary to investigate possible differences in the trajectory shape and the velocity profile during discrete and cyclical movements and how specific components of discrete movements, such as motion termination (Dounskaia et al. 2005), contribute to these differences.

Second, the model was limited to planar two-joint movements, which was necessary to derive explicit analytical expressions for the KIs. Would the KIs be observed when additional degrees of freedom are included in motion? Apparently, values of the KI parameters would differ from those predicted by the obtained formulae because the kinematic structure of the arm would be different. Moreover, some KIs are likely to be violated. Experimental support for this possibility with respect to the power law has been provided by Schaal and Sternad (2001). The bell (dome) shape of the velocity profile is a robust KI that is likely maintained when a degree of freedom is added; however, only if all degrees of freedom change synchronously in the sinusoidal-like fashion. An additional degree of freedom would violate trajectory straightness during point-to-point movements performed with sinusoidal joint motions. This can be demonstrated analytically with use of simple considerations of velocity vectors similar to those presented in Fig. 3. It can be shown with this method that if the arm end-point moves along a straight line, adding a degree of freedom, such as wrist or humeral rotation, disrupts the trajectory straightness.

The third limitation of the model is that it addresses only periodic motion near the center of the arm's practical workspace. In terms of joint kinematics, this limitation implies a requirement for smooth, sinusoidal-like motions of moderate amplitudes. Violations of this requirement would differentially affect the three KIs. The properties of the 1/3-power function in (9) suggest that the power law would be valid for a wide range of smooth joint motions. This is in agreement with reported examples of movements that follow the power law and that emerge from smooth but not strictly biphasic sinusoidal joint motions of constant amplitude (Viviani and Flash 1995). However, the requirement for moderate but not small joint amplitudes might be critical for this KI, again, due to the properties of the 1/3-power function. The sinusoidal-like joint motions are probably important for a smooth single-peak velocity profile, whereas the size of joint amplitudes is not critical. The model predicts straight trajectory for sinusoidal joint motions of small amplitude. This, however, does not exclude a possibility that non-sinusoidal joint motions can also result in relatively straight trajectories. For instance, drawing the horizontal and right-tilted line in the present experiment included non-sinusoidal motion at one joint. Although end-point trajectory was less straight for these lines as compared with the other two lines, it still looked close to a straight line. Thus, the model does not completely clarify the conditions for violation of this KI, although this clarification would rely on a definition of a curvature threshold under which a trajectory can still be considered straight.

Although some of the KIs might be maintained when joint motions are not strictly sinusoidal, overall, the presented results suggest that the KIs in end-point motion are usually associated with smooth sinusoidal-like joint motions of moderate amplitudes. Thus, instead of the three KIs of end-point kinematics, a single KI of sinusoidal joint motions can be considered. Although sinusoidal joint motions have often been reported (Bernstein 1984; Buchanan et al. 1997; Schaal and Sternad 2001; Soechting and Lacquaniti 1986; Soechting and Terzuolo 1987; Sternad and Schaal 1999), little research has addressed the reasons for their emergence. Schaal and Sternad (2001) discussed central pattern generators as a possible mechanism underlying sinusoidal joint movements. Another possibility that stems from the study by Gribble et al. (1996) is that spring-like properties of muscles contribute to sinusoidal joint movements. This hypothesis is supported by a consideration that force produced by spring-like muscles is proportional to muscle length. Such force would generate the same type of single-joint movement as motion of a pendulum in the gravitational force field, which is sinusoidal.

Thus, the KIs of end-point kinematics might be by-products of a number of factors that cause sinusoidal joint motions. However, it is also possible that sinusoidal joint motions are, at least partially, a consequence of incorporation of the three KIs in end-point trajectories at the level of central control. The voluntary origin of the KIs is evident from a consideration that movement goals can, in principle, be achieved without the KIs. For instance, it is possible to move along a curve instead of the straight path during pointing, to produce velocity of other than the bell shape, and to perform a curvilinear movement that does not follow the power law. Furthermore, the KIs do not "automatically" emerge in end-point motion but likely require a substantial effort to be learned and maintained. For instance, path straightness and smooth bell-shaped velocity profiles are not observed in movements of infants at the early stages of reaching acquisition and are progressively developed with extensive practice (Berthier et al. 1999; Konczak et al. 1997; Konczak and Dichgans 1997; Thelen et al. 1993; Von Hofsten 1991). Multiple velocity peaks and deviations from the straight path are often observed in reaching movements of patients with motor disorders that have a central origin (Alberts 2000; Bastian et al. 1996; Castiello et al. 2000; Flash et al. 1992; Levin 1996; Massaquoi and Hallet 1996).

The production of end-point trajectories characterized by the KIs might have various reasons. For instance, it is possible that there is a tendency to provide straightness of the visual representation of trajectory during point-to-point movements (Miall and Haggard 1995; Wolpert et al. 1995) because it simplifies visual images of movements and improves predictability and controllability of motor performance. Also, it is possible that the KIs are exploited to simplify neural coding of arm movements, which is supported by observations of the power law in the cortical representation of drawing movements (Schwartz 1994; Schwartz and Moran 1999, 2000).

Thus, it is possible that the KIs emerge due to sinusoidal joint motions, but it is also possible that sinusoidal joint motions emerge due to the KIs. There is a third alternative that both the KIs and sinusoidal joint motions are by-products of a single factor, for example, of an optimal control strategy. A number of relevant optimization criteria have been proposed. Some of them address properties of end-point trajectory, such as minimal jerk, maximal smoothness, and minimal noise (Flash and Hogan 1985; Harris and Wolpert 1998; Richardson and Flash 2002; Schaal and Sternad 2001; Todorov and Jordan 1998; Viviani and Flash 1995). Energy-related minimization criteria can also result in the KIs (Lebedev et al. 2001) as well as in sinusoidal joint motions because

they are likely to minimize energy expenses, as suggested by the consideration that motion of a free pendulum is a sinusoid of the resonance frequency. Optimality of sinusoidal joint movements in terms of energy expenditure is also supported by the finding that the preferred gait patterns are rhythmic movements associated with minimal levels of metabolic and mechanical energy consumption (Diedrich and Warren 1995). All these optimization criteria likely result in sinusoidal joint motions (and hence, in the KIs) similar to how during translational motion of a material point, the straight path yields minimization of various cost functions, including movement time, distance, jerk, performed work, and energy expenditure.

While research has been striving for distinguishing a single factor that fully accounts for the KIs, it is also possible that the KIs are a result of a harmonious combination of various factors that compliment each other to facilitate movement performance simultaneously at different levels of the motor system. While the KIs might simplify cognitive aspects of movement control, such as planning and examination of performance, and ensure smooth and accurate movements of the end-point, the human musculoskeletal system might have been adjusted in evolution to provide these kinematic characteristics with minimal energy expenditure (Marzke and Marzke 2000).

In conclusion, a planar two-joint model of cyclical arm movements was derived to analytically predict a number of regularities (kinematic invariants, KIs) that have often been experimentally observed in end-point trajectories. The model predicts the power law during drawing movements, and the straight path and the dome shape of the velocity profile during point-to-point movements. It demonstrates that all three KIs are associated with the planar two-joint approximation of the arm kinematics and with sinusoidal-like motions at the joints. Explicit analytical expressions are obtained for two KIs, the power law and the dome shape of the velocity profile, that specify the quantitative dependence of these KIs on parameters of arm kinematics and sinusoidal joint motions. This creates a mechanism for experimentally testable predictions about variations in end-point motion characteristics across various movement conditions and subject groups.

Appendix A: Approximation of the gain factor *K* with a constant

Inserting (5) and (6) in (9) and using (2) and (3) results in

$$K = (|F_1 + F_2|)^{1/3}, \tag{A1}$$

where

$$F_1 = \omega^3\left[l_p l_d A_p A_d \sin(\alpha_d + A_d \sin(\omega t + \theta)) \sin(\theta)\right] \tag{A2}$$

and

$$\begin{aligned} F_2 = {} & l_p^2 A_p^3 \cos^3(\omega t) + l_d^2 (A_p + A_d)^3 \\ & \times (\cos(\omega t) + \cos(\omega t + \theta))^3 + \\ & + l_p l_d \cos(\alpha_d + A_d \sin(\omega t + \theta)) \left\{A_p (A_p + A_d)\right. \\ & \times \left.\left[(A_p + A_d)(\cos(\omega t) + \cos(\omega t + \theta)) + A_p \cos(\omega t)\right]\right\}. \end{aligned} \tag{A3}$$

When A_d and A_p are small, K can be estimated by $K = \omega(l_p l_d A_p A_d \sin(\alpha_d) \sin(\theta))^{1/3}$. Indeed, when A_d and A_p decrease, F_1 can be approximated by a constant $R = \omega^3\left[l_p l_d A_p A_d \sin(\alpha_d) \sin(\theta)\right]$ because α_d is usually not close to 0 or to π during human movements, and therefore, variations in $\sin(\alpha_d + A_d \sin(\omega t + \theta))$ are small. F_2 is a periodic function that varies around zero. Although both F_1 and F_2 decrease when A_p and A_d decrease, F_2 decreases faster than F_1 because F_1 depends on the second power of the joint amplitudes and F_2 depends on the third power of joint amplitudes. For this reason, K can be approximated as $K^* = F_1^{1/3}$.

Appendix B: Dependence of end-point velocity on joint coordination pattern

Prediction 4 follows from (13) when $\cos(\omega t) = 1$ and the term $L^2 + l_d^2 - l_p^2$ is substituted by $2 l_p l_d \cos(\beta)$, where β is the angle between the distal segment and the line SE (see Fig. 1). Then V_{peak} can be expressed as

$$V_{\text{peak}} = \omega\sqrt{L^2 A_d^2 + l_p^2 A_p^2 \pm 2 L l_d A_d A_p \cos(\beta)}. \tag{B1}$$

When joint amplitudes are small, the distance L between the shoulder joint S and the end-point E is approximately constant. Then V_{peak} in (B1) is higher for $\theta = 0$ ("+" under the radical) than for $\theta = \pi$ ("−" under the radical) because β is always less than $\pi/2$ during movements of the human arm. This property of the angle β follows from the second triangle theorem that yields a relationship

$$\sin(\beta) = (l_p / l_d) \sin(\psi), \tag{B2}$$

where ψ is the angle between the upper arm and SO. The changes in the angle ψ are limited by 0 and π when the elbow rotates from full extension to full flexion, which provides an inequality

$$0 \leqslant \sin(\beta) \leqslant l_p / l_d. \tag{B3}$$

With use of segment lengths $l_p = 0.18H$ and $l_d = 0.244H$ (see Sect. 2), (B1) and (B2) result in the limits $0 \le \beta \le 0.78$ (47.5°) for all possible arm configurations. Thus, $\cos(\beta)$ is always positive, and therefore, endpoint velocity is higher when the two joints simultaneously flex or extend than when they move anti-phase.

Appendix C: Dependence of movement distance on joint coordination pattern

It is demonstrated in this appendix that sinusoidal movements (3) at the shoulder and elbow result in longer movement distance when $\theta = 0$ than when $\theta = \pi$.

Distance D between a position (x_1, y_1) of the endpoint defined by the joint angles $\gamma_{p1} = \alpha_p + \varphi_{p1}$ and $\gamma_{d1} = \alpha_d + \varphi_{d1}$ and a position (x_2, y_2) when the joint angles are $\gamma_{p2} = \alpha_p + \varphi_{p2}$ and $\gamma_{d2} = \alpha_d + \varphi_{d2}$, respectively, is computed from $D^2 = \Delta x^2 + \Delta y^2$, where $\delta x = x_2 - x_1$ and $\delta y = y_2 - y_1$. Expressions for Δx and Δy obtained from (4) are

$$\begin{aligned}\Delta x &= l_p \cos\left(\alpha_p + \varphi_{p2}\right) + l_p \cos\left(\alpha_p + \alpha_d + \varphi_{p2} + \varphi_{d2}\right) \\ &\quad - l_p \cos\left(\alpha_p + \varphi_{p1}\right) - l_p \cos\left(\alpha_p + \alpha_d + \varphi_{p1} + \varphi_{d1}\right), \\ \Delta y &= l_p \sin\left(\alpha_p + \varphi_{p2}\right) + l_p \sin\left(\alpha_p + \alpha_d + \varphi_{p2} + \varphi_{d2}\right) \\ &\quad - l_p \sin\left(\alpha_p + \varphi_{p1}\right) - l_p \sin\left(\alpha_p + \alpha_d + \varphi_{p1} + \varphi_{d1}\right).\end{aligned} \tag{C1}$$

Expansion of the sine and cosine functions in (C1) in the Taylor series around α_p and $\alpha_p + \alpha_d$, respectively, yields

$$\begin{aligned}D^2 = \Delta x^2 + \Delta y^2 &= l_p^2\left(\varphi_{p2} - \varphi_{p2}\right)^2 \\ &\quad + l_d^2\left(\varphi_{p2} + \varphi_{d2} - \varphi_{p1} - \varphi_{d1}\right)^2.\end{aligned} \tag{C2}$$

When the sinusoidal approximations (3) of joint movements are used, one target is achieved when $\omega t = \pi(2k+1/2)$ and the other target is achieved when $\omega t = \pi(2k+3/2)$, where $k = 1, 2, \ldots$. Using these values, it can be shown that

$$D^2 = 4l_p^2 A_p^2 + 4l_d^2\left(A_p + A_d\right)^2, \quad \text{when } \theta = 0, \tag{C3}$$

and

$$D^2 = 4l_p^2 A_p^2 + 4l_d^2\left(A_p - A_d\right)^2, \quad \text{when } \theta = \pi. \tag{C4}$$

Comparison of (C3) and (C4) demonstrates that the distance D is longer when $\theta = 0$ than when $\theta = \pi$. Since this result was obtained with use of the Taylor series expansion, it is valid for small amplitudes of joint movements.

Acknowledgments I thank Dr. Yury Shimansky, Dr. Sergey Nikitin, and the anonymous reviewer for helpful suggestions on the manuscript. The study was supported by NIH grant NS43502.

References

Adam JJ, van der Bruggen DPW, Bekkering H (1993) The control of discrete and reciprocal target-aiming responses: evidence for the exploitation of mechanics. Hum Mov Sci 12:353–364

Alberts JL, Saling M, Adler CH, Stelmach GE (2000) Disruptions in the reach-to-grasp actions of Parkinson's patients. Exp Brain Res 134:353–62

Atkeson CG, Hollerbach JM (1985) Kinematic features of unrestrained vertical arm movements. J Neurosci 5:2318–2329

Bastian AJ, Martin TA, Keating JG, Thach WT (1996) Cerebellar ataxia: abnormal control of interaction torques across multiple joints. J Neurophysiol 76:492–509

Bernstein N (1984) Biodynamics of locomotion. In: Writing HTA (ed) Human motor actions: Bernstein reassessed. North-Holland, Amsterdam, pp 171–222

Berthier NE, Clifton RK, McCall DD, Robin DJ (1999) Proximodistal structure of early reaching in human infants. Exp Brain Res 127:259–269

Buchanan JJ, Park JH, Ryu YU, Shea CH (2003) Discrete and cyclical units of action in a mixed target pair aiming task. Exp Brain Res 150:473–489

Buchanan JJ, Park JH, Shea CH (2004) Systematic scaling of target width: dynamics, planning, and feedback. Neurosci Lett 367:317–322

Buchanan JJ, Kelso SA, de Guzman GC (1997) Self-organization of trajectory formation. I. Experimental evidence. Biol Cybern 76:257–273

Castiello U, Bennett KMB, Bonfiglioli C, Peppard RF (2000) The reach-to-grasp movement in Parkinson's disease before and after dopaminergic medication. Neuropsychologia 38:54–59

Chaffin DB, Andersson GBJ (1984) Occupational biomechanics. Wiley, New York

De'Sperati C, Viviani P (1997) The relationship between curvature and velocity in two-dimensional smooth pursuit eye movements. J Neurosci 17:3932–3945

Diedrich FJ and Warren WH (1995) Why change gaits-dynamics of the walk run transition. J Exp Psychol Hum Percept Perform 21:183–202

Dounskaia N, Ketcham CJ, Stelmach GE (2002a) Commonalities and differences in control of a large set of drawing movements. Exp Brain Res 146:11–25

Dounskaia N, Ketcham CJ, Stelmach GE (2002b) Influence of biomechanical constraints on horizontal arm movements. Motor Control 6:366–387

Dounskaia N, Wisleder D, Johnson TA (2005) Influence of biomechanical factors on substructure of pointing movements. Exp Brain Res 164:505–516

Flash T, Hogan N (1985) The coordination of arm movements: an experimentally confirmed mathematical model. J Neurosci 7:1688–1703

Flash T, Inzelberg R, Schectman E, Korcyzn AD (1992) Kinematic analysis of upper limb trajectories in Parkinson's disease. Exp Neurol 118:215–26

Fitts PM (1954). The information capacity of the human motor system in controlling the amplitude of movement. J Exp Psychol 47:381–391

Georgopoulos AP, Kalaska JF, Massey JT (1981) Spacial trajectories and reaction times of aimed movements: effects of practice, uncertainty, and change in target location. J Neurophysiol 46:725–743

Graham KM, Moore KD, Cabel DW, Gribble PL, Cisek P, Scott SH (2003) Kinematics and kinetics of multijoint reaching in nonhuman primates. J Neurophysiol 89:2667–2677

Gribble PL, Ostry DJ (1996) Origins of the power law relation between movement velocity and curvature: modeling the effects of muscle mechanics and limb dynamics. J Neurophysiol 76:2853–2860

Guiard Y (1993) On Fitts's and Hooke's laws: simple harmonic movement in upper limb cyclical aiming. Acta Psychologica 82:139–159

Guiard Y (1997) Fitts' law in the discrete vs. cyclical paradigm. Hum Mov Sci 16:97–131

Haggard P, Richardson J (1996) Spatial patterns in the control of human movement. J Exp Psychol Hum Percept Perform 22: 42–62

Harris CM, Wolpert DM (1998) Signal-dependent noise determines motor planning. Nature 34:780–784

Hogan N (1984) An organizing principle for a class of voluntary movements. J Neurosci, 4:2745–2754

Hogan N (1985) The mechanics of multi-joint posture and movement control. Biol Cybern 52:315–331

Jordan MI, Flash T, Arnon Y (1994) A model of the learning of arm trajectories from spatial deviations. J Cognit Neurosci 6:359–376

Konczak J, Dichgans J (1997) The development toward stereotypic arm kinematics during reaching in the first 3 years of life. Exp Brain Res 117:346–354

Konczak J, Borutta M, Topka H, Dichgans J (1997) The development of goal-directed reaching in infants. Exp Brain Res 113:465–474

Lacquaniti F, Terzuolo CA, Viviani P (1983) The law relating kinematic and figural aspects of drawing movements. Acta Psychologica 54:115–130

Lebedev S, Tsui WH, Van Gelder P (2001) Drawing movements as an outcome of the principle of least action. J Math Psychol 45:43–52

Levin MF (1996) Interjoint coordination during pointing movements is disrupted in spastic hemiparesis. Brain 119:281–293

Marzke MW, Marzke RF (2000) Evolution of the human hand: approaches to acquiring, analysing and interpreting the anatomical evidence. J Anat 197:121–40 (Review)

Massaquoi S, Hallet M (1996) Kinematics of initiating a two-join arm movement in patients with cerebellar ataxia. Can J Neurol Sci 23:3–14

Massey J, Lurito J, Pellizzer G, Georgopoulos A (1992) Three-dimensional drawings in isometric conditions: relation between geometry and kinematics. Exp Brain Res 88:685–690

Miall RC, Haggard PN (1995) The curvature of human arm movements in the absence of visual experience. Exp Brain Res 103:421–428

Morasso P (1981) Spacial control of arm movements. Exp Brain Res 42:223–227

Nelson W (1983) Physical principles for economies of skilled movements. Biol Cybern 46:135–147

Pollick FE, Ishimura G (1996) The three-dimensional curvature of straight ahead movements. J Mot Behav 28:271–279

Richardson MJE, Flash T (2002) Comparing smooth arm movements with the two-thirds power law and the related segmented-control hypothesis. J Neurosci 22:8201–8211

Schaal S, Sternad D (2001) Origins and violations of the 2/3 power law in rhythmic three-dimensional arm movements. Exp Brain Res 136:60–72

Schwartz A (1994) Direct cortical representation of drawing. Science 265:540–542

Schwartz AB, Moran DW (1999) Motor cortical activity during drawing movements: population representation during leminiscate tracing. J Neurophysiol 82:2705–2718

Schwartz AB, Moran DW (2000) Arm trajectory and representation of movement processing in motor cortical activity. Eur J Neurosci 12:1851–1856

Soechting JF, Lacquaniti F (1981) Invariant characteristics of a pointing movement in man. J Neurosci 1:710–720

Soechting JF, Terzuolo CA (1987) Sensorimotor transformations underlying the organization of arm movements in three-dimensional space. Can J Physiol Pharmacol 66:502–507

Soechting JF, Lacquaniti F& Terzuolo CA (1986) Coordination of arm movements in three dimentional space. Sensorimotor mapping during drawing movement. Neurosci 17:295–311

Sternad D, Schaal S (1999) Segmentation of endpoint trajectories does not imply segmented control. Exp Brain Res 124: 118–136

Thelen E, Corbetta D, Kamm K, Spenser JP, Schneider K, Zernicke RF (1993) The transition to reaching: mapping intention and intrinsic dynamics. Child Dev 64:1058–1098

Todorov E, Jordan MI (1998) Smoothness maximization along a predefined path accurately predicts the speed profiles of complex arm movements. J Neurophysiol 80:696–714

Viviani P, Cenzato M (1985) Segmentation and coupling in complex movements. J Exp Psychol Hum Percept Perform 11: 828–845

Viviani P, Flash T (1995) Minimum-jerk, two-third power law and isochrony: converging approaches to movement planning. J Exp Psychol 21:32–53

Viviani P, Schneider R (1991) A developmental study of the relation between geometry and kinematics in drawing movements. Neurosci 10:211–218

Viviani P, Terzuolo CA (1982) Trajectory determines movement dynamics. Neurosci 7:431–437

Von Hofsten C (1991) Structuring of early reaching movements: a longitudinal study. J Mot Behav 23:280–292

Wolpert DM, Ghahramani Z, Jordan MI (1995) Are arm trajectories planned in kinematic or dynamic coordinates? An adaptation study. Exp Brain Res 103:460–470